Nucleic Acids Research, 2005, Vol. 33, No. 13 ***4223–4234***
doi:10.1093/nar/gki726

Intercalator conjugates of pyrimidine locked nucleic acid-modified triplex-forming oligonucleotides: improving DNA binding properties and reaching cellular activities

Erika Brunet, Maddalena Corgnali[1], Loïc Perrouault, Victoria Roig[2], Ulysse Asseline[2], Mads D. Sørensen[3], B. Ravindra Babu[3], Jesper Wengel[3] and Carine Giovannangeli*

Laboratoire de Biophysique, Museum national d'Histoire naturelle USM 0503, CNRS UMR 5153, INSERM U 565, 43 rue Cuvier, 75005 Paris, France, [1]Dipartimento di Scienze e Tecnologie Biomediche, Universita degli Studi di Udine, 33100 Udine, Italy, [2]Centre de Biophysique Moléculaire, CNRS UPR4301, Rue Charles Sadron, 45071 Orléans Cedex 2, France and [3]Nucleic Acid Center, Department of Chemistry, University of Southern Denmark, Campusvej 55, DK-5230 Odense M, Denmark

Received May 13, 2005; Revised and Accepted July 5, 2005

ABSTRACT

Triplex-forming oligonucleotides (TFOs) are powerful tools to interfere sequence-specifically with DNA-associated biological functions. (A/T,G)-containing TFOs are more commonly used in cells than (T,C)-containing TFOs, especially C-rich sequences; indeed the low intracellular stability of the non-covalent pyrimidine triplexes make the latter less active. In this work we studied the possibility to enhance DNA binding of (T,C)-containing TFOs, aiming to reach cellular activities; to this end, we used locked nucleic acid-modified TFOs (TFO/LNAs) in association with 5′-conjugation of an intercalating agent, an acridine derivative. *In vitro* a stable triplex was formed with the TFO-acridine conjugate: by SPR measurements at 37°C and neutral pH, the dissociation equilibrium constant was found in the nanomolar range and the triplex half-life ~10 h (50-fold longer compared with the unconjugated TFO/LNA). Moreover to further understand DNA binding of (T,C)-containing TFO/LNAs, hybridization studies were performed at different pH values: triplex stabilization associated with pH decrease was mainly due to a slower dissociation process. Finally, biological activity of pyrimidine TFO/LNAs was evaluated in a cellular context: it occurred at concentrations ~0.1 μM for acridine-conjugated TFO/LNA (or ~2 μM for the unconjugated TFO/LNA) whereas the corresponding phosphodiester TFO was inactive, and it was demonstrated to be triplex-mediated.

INTRODUCTION

Molecules able to specifically recognize predetermined sequences in the DNA double helix are appropriate to modulate DNA-associated biological functions. Triplex-forming oligonucleotides (TFOs) bind in the major groove of oligopyrimidine•oligopurine sequences allowing specific targeting of the double-stranded DNA. The TFO can form Hoogsteen or reverse Hoogsteen hydrogen bonds with the purine-containing strand of the double helix, depending on the nature of the target sequence. Structural requirements influence the design of TFOs and has lead to the classification in different subtypes with individual binding properties (1). TFOs containing C and T nucleotides (also named pyrimidine TFOs) bind in parallel orientation via Hoogsteen hydrogen bonds [(T,C)-motif] and their binding decreased at physiological pH since cytosines must be protonated to support a second hydrogen bond; TFOs containing G and A or T nucleotides [(G,A)- and (G,T)-motifs] bind mainly in anti-parallel orientation via reverse Hoogsteen bonds and their binding is disfavored by intracellular concentration of potassium since they can be involved in auto-association processes that could compete with triplex formation and induce additional interactions with specific proteins, leading to side effects in cells. However, TFOs have been successfully used as DNA code-reading molecules *in vitro* and in cells, and triplex formation has been demonstrated to interfere in a sequence-specific manner with biological

*To whom correspondence should be addressed. Tel: +33 1 40 79 37 11; Fax: +33 1 40 79 37 05; Email: giovanna@cimrs1.mnhn.fr

functions occurring on DNA, namely transcription (initiation and elongation), replication, repair and recombination, and has also been useful to guide molecules acting on DNA unspecifically, such as DNA damaging agents [for reviews see (2,3)]. For all triplex-based applications in cells, pyrimidine TFOs, especially C-rich sequences, have been demonstrated to be only weakly active, and G-containing TFOs are therefore the most commonly used TFOs. Yet a remaining key challenge to be addressed is the current low efficiency of TFO-induced activities in cells. One approach consists in improvement of the ability of TFOs to form a stable complex in a cellular context. To reach this goal, many efforts have been focused on developing chemically modified oligonucleotides. Among them, locked nucleic acids (LNA) that contain ribonucleotides with a 2′-*O*,4′-C-methylene linkage have been synthesized as described previously (4,5). LNA-containing TFOs have been recently described to effect very significant triplex stabilization. Previous works have thus shown that alternating LNA and DNA nucleotides in TFO sequences is appropriate for triplex formation (6,7). In this context, *in vitro* favorable binding properties of pyrimidine LNA-modified TFOs (TFO/LNAs) have been reported, providing evidence that LNA-induced triplex stabilization compared to the non-modified TFO is associated with a reduced entropic barrier (most probably due to appropriate preorganization of the TFO/LNA) and a slower dissociation rate constant (8). To date, pyrimidine TFO/LNAs have been used only for *in vitro* applications (9). Still, LNA-modified oligonucleotides are promising molecules, even for *in vivo* applications, as supported by their use as antisense agents (10,11). Alternatively, TFO-intercalator conjugates have been synthesized. The most commonly used intercalators are acridine (Acr) and psoralen (Pso) derivatives, the latter being mainly used in association with irradiation, as a photoactive DNA cross-linker. It is established that they stabilize the triplex when attached at the end of the TFO, most probably by preferential intercalation at the duplex–triplex junction (12). In fact, a few hybridization studies of such conjugates have been reported so far. It has been shown that the triplex stabilization induced by the intercalating agent can be observed in different contexts, such as different TFO chemistries (phosphodiester, phosphorotioate, phosphoramidate, 2′-*O*-methyl sugars) as well as different TFO binding motifs [(T, C)-, (T, G)- or (A, G)-containing TFOs] (13–15). Furthermore, either the 5′ or the 3′ end of TFOs can be conjugated with appropriate linkers attached to intercalator (16). Using this approach, increase in triplex stability has been described, but only using gel shift assays (for determination of the concentration necessary for 50% triplex formation) or UV melting experiments (for determination of melting temperature, T_m). In cellular applications, intercalating agents have been attached to TFOs (phosphodiester and backbone or sugar-modified) and the corresponding conjugates have been shown to exhibit biological activity (17–19).

In the present work the objectives are to evaluate the triplex-forming properties and intracellular activities of pyrimidine TFO/LNAs conjugated or not to an acridine derivative, used as a model of a DNA intercalating agent. We have for the first time characterized the kinetic origins of triplex stabilization induced by acridine conjugation. The pH-dependence of pyrimidine TFO/LNA binding was also explored. To study these aspects, surface plasmon resonance (SPR) biosensor technology was used to evaluate kinetic parameters of triplex formation. Finally, we determined the ability of the TFO/LNAs to interfere with DNA acting proteins *in vitro* and in cells, and we used experimental systems designed to demonstrate a triplex-based mechanism and to evaluate the advantage of pyrimidine TFO/LNAs. We provide evidence of biological activities of pyrimidine TFO/LNAs in a cellular context, as monitored by inhibition of transcription elongation, under conditions where the parent phosphodiester TFOs were inactive. The TFO/LNA-acridine conjugate was active at submicromolar concentrations (~0.1 μM) and the unconjugated TFO/LNA in the micromolar range (~2 μM); to our knowledge, such efficiency in cellular triplex-based activities has never been reported previously for any pyrimidine C-rich TFO. Our results encourage further developments of TFO/LNAs to interfere with DNA metabolism.

MATERIALS AND METHODS

Oligonucleotides

Oligonucleotide analogues with LNA residues were synthesized as described previously (4) or purchased from Proligo (France SAS). For cellular experiments, the phosphodiester oligonucleotide (Acr-16TC/po, sequence in Figure 1) was 3′-modified by incorporation of a propylamine group (named Acr-16TC$^{\$}$/po) to resist nuclease-mediated degradation.

The covalent attachment of acridine to the 5′ end of 16TC/LNA and 16py(2)/LNA TFOs was achieved by the reaction of 2-methoxy-6-chloro-9-(ω-bromohexylamino)-acridine (20) with 5′-thiophosphorylated 16TC/LNA and 16py(2)/LNA sequences (purchased from Proligo) by a method adapted from a previously reported procedure (21). Lyophilized ODNs (sp-16TC/LNA or sp-16py(2)/LNA) (20 OD units) were dissolved in MeOH (1 ml) in the presence of

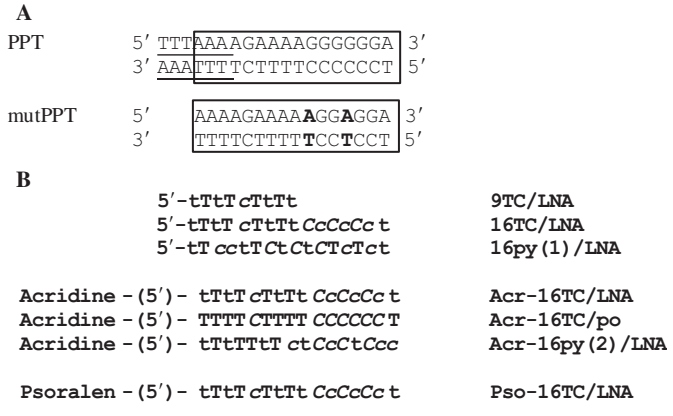

Figure 1. Sequences of the oligopyrimidine•oligopurine DNA targets (**A**) and of the oligonucleotides (**B**) used in this study. (A) The wild-type PPT target sequence (boxed), Dra I recognition site (underlined) are shown, as well as the mutated PPT duplex presenting two mutations (in bold). (B) (T,C)-containing TFOs directed against the wild-type PPT duplex and control sequences. Small letters indicate LNA nucleotides and capitals DNA nucleotides. Cytosines in italic (*C* and *c*) are methylated at position 5; all cytosines (LNA and DNA) are 5-methylated. The abbreviated names are indicated near the sequences. (po) stands for phosphodiester. Last four TFOs are either acridine (Acr) or psoralen (Pso) 5′-conjugated TFO/LNAs.

18-Crown-6-ether (0.010 *g*) and the acridine derivative (0.002 *g*) dissolved in MeOH (0.5 ml) was added. The mixture was incubated with stirring at room temperature for 24 h and then concentrated to dryness. 1 M sodium phosphate buffer (1 ml), pH 6, was added and the excess of acridine derivative was extracted from CH_2Cl_2 (3 × 3 ml). The crude conjugates were purified by reversed-phase chromatography using a Licrhospher 100 RP 18 (5 μm) column (12.5 × 4 mm^2; Merck) and a linear gradient of CH_3CN (5–35% in 40 min) in 0.1 M TEAA, pH 7, buffer with a flow rate of 1 ml/min. Conjugates were eluted with retention times 10 min longer than those of the corresponding 5′-thiophosphorylated TFOs. The conjugates Acr-16TC/LNA and Acr-16py(2)/LNA were characterized by UV absorption spectroscopy and electrospray mass spectrometry analysis. Acr-16TC/LNA: Found: 5485.81 ± 0.77 (calculated: 5487.27 for $C_{189}H_{238}ClN_{41}O_{115}P_{16}S$). Acr-16py (2)/LNA: Found: 5485.79 ± 0.94 (calculated: 5487.27 for $C_{189}H_{238}ClN_{41}O_{115}P_{16}S$).

Plasmids

The pSP-F47 plasmid was constructed by insertion of a 780 bp fragment of the HIV-1/*nef* gene containing the oligopyrimidine•oligopurine PPT target sequence, between the T_7 and SP_6 promoters, in the pSP73 host vector (Promega), as previously described in details (22). This system allows to run bidirectional *in vitro* transcription assays.

The (+)PPT/luc and (+)mutPPT/luc plasmids contain the firefly luciferase (*Photinus pyralis*) under the control of the murine phosphoglycerate kinase (PGK) promoter. A 34 bp insert [5′-CCACTTTTT(PPT or mutPPT)CTGGAAGGG-3′] containing the wild-type HIV-1 oligopurine tract (PPT: 5′-AAAAGAAAAGGGGGGA-3′) or a mutated version (mutPPT: 5′-AAAAGAAAAA**G**GA**A**GA-3′, 2 mutations in bold) was cloned on the 5′-transcribed sequence of the luciferase gene in the (+)PPT/luc or (+)mutPPT/luc, 113 bp downstream of the PGK start site. These constructs have been described in more details (15).

The pRL-TK vector (Promega) contains the *Renilla* luciferase (RL, from the marine organism *Renilla reniformis*) under the control of the TK promoter. pRL-TK was used to monitor transfection efficiency.

Electrophoresis mobility shift assay

PPT or mutPPT hairpin intramolecular duplexes were 5′ end-labeled with [γ-^{32}P]ATP (3000 Ci/mmol, Amersham Pharmacia Biotech.) by T4 polynucleotide kinase (Promega). The duplex (2 nM) was incubated with increasing concentrations of TFO in a buffer containing 50 mM HEPES pH 7.2, 150 mM NaCl, 1 mM $MgCl_2$, 0.5 mM spermine, 0.1 μg shared salmon sperm DNA and 10% sucrose. The non-denaturing polyacrylamide gel (15%) was run at 37°C in a buffer containing 50 mM HEPES pH 7.2 and 1 mM $MgCl_2$. Gels were scanned with phosphorimager and results quantified (±5%) using the Image-Quant software (Molecular Dynamics). The level of complex formation was estimated by the TFO concentration where 50% of the complex was formed (C_{50}).

UV absorption melting experiments

All thermal denaturation experiments were performed in a 10 mM sodium cacodylate buffer (at the indicated pH value) containing either 10 mM $MgCl_2$ and 150 mM NaCl, or 100 mM NaCl. The sample contained 1 μM duplex (PPT or mutPPT duplex: 29 bp long intramolecular hairpin duplexes) and 1.5 μM TFO (see sequences in Figure 1). Melting profiles were recorded at 260 nm, using an UVIKON 940 spectrophometer, as already described (23). Corrections for spectrophotometric instability were made by subtracting the absorbance at 405 nm from that at 260 nm. The temperature was decreased from 92 to 0°C and increased again to 92°C at a rate of 0.2°C/min. All the cooling and heating profiles presented here were reversible except in the case presented in Figure S1. The melting temperature (T_m in °C) was determined from melting curves, both directly and after subtraction of the duplex absorption from that of the triplex. The triplex T_m was estimated within (±) 0.5°C accuracy, except when the melting profiles of triplex transition presented a hysteresis [(±)1.5°C accuracy in T_m].

SPR experiments

SPR measurements were performed on a BIAcore 2000™ (BIAcore AB, Sweden) using a carboxymethylated dextran-coated sensor chip (CM5), as previously described (24). Briefly, one micromolar solutions of 3′-biotinylated hairpin duplexes (PPT duplex and control duplex 5′-GCTAAAGAGAGAGAGAAATCGTTTTCGATTCTCTCTCTCTTTAGCTTTTTT-Biotin) were prepared in a buffer containing 10 mM HEPES pH 7.4, 0.15 M NaCl, 3 mM EDTA and 0.0005% surfactant P20; purchased by BIAcore) and duplex injection was controlled to obtain a 1500 RU increase. Serial dilutions of TFO were prepared in 10 mM sodium cacodylate, with either 10 mM $MgCl_2$, 150 mM NaCl, or 100 mM NaCl, and 0.0005% surfactant P20 at pH 6.5 or 7. These triplex-forming buffer conditions are the same as the ones used in UV absorption melting experiments. Serial TFO injections were performed simultaneously on the hairpin duplex containing the target PPT sequence and on the control duplex lacking the PPT sequence. All the sensor grams were corrected by subtraction of the control duplex signal, reflecting mainly bulk index changes. A typical sensor gram was shown in Figure S2.

The sonograms were analyzed using the BIAevaluation 3.0 software. The association rate constant k_{on} was determined by the linear fitting of the apparent association rate constant [$k_{app} = k_{on} \times (TFO) + k_{off}$] at different TFO concentrations, in agreement with a two-state model; for k_{on}, experimental error was (±) 15%. Noteworthy, concerning the dissociation process, for the acridine-conjugated TFO/LNA (Acr-16TC/LNA), it was very slow under our experimental conditions and k_{off} values were likely overestimated since the dissociation half-life of the triplex was long compared to the analysis time (∼2 h). The mass transport effects were negligible under our experimental conditions.

Restriction enzyme (Dra I) protection assay

The pCMV(+)PPT/luc plasmid contains the PPT sequence overlapping one of the 7 Dra I sites [for detailed description, see (25)]. It was used as a substrate for a restriction enzyme protection assay. For the cleavage assay, the pCMV(+)PPT/luc plasmid was incubated at 37°C for 20 min, with increasing amounts of oligonucleotides in 50 mM HEPES pH 7.2, 50 mM NaCl, 10 mM $MgCl_2$ and 0.5 mM spermine in the presence of

Dra I enzyme. The fragments generated by Dra I cleavage in absence of TFO are 1936, 1718, 692, 683, 534 and 19 bp long. A 3654 bp fragment corresponding to the addition of the 1936 and the1718 bp fragments was obtained when TFO-induced inhibition of Dra I cleavage occured. The extent of triplex-mediated inhibition of Dra I cleavage was assessed by gel electrophoresis (0.8% agarose gel) and quantified (with an estimated error of (±) 5%). The TFO concentration giving 50% inhibition (IC_{50}) was then evaluated.

In vitro transcription assay

Transcription assays were performed using the pSP-F47 plasmid that contains the PPT sequence between T_7 and SP_6 promoters. The plasmid was linearized by BspE 1 for T_7 transcription and synthesis of purine/PPT-containing RNA (660 nt long), or by Bsu36 I for synthesis of pyrimidine/PPT-containing RNA (597 nt long). The linearized plamids (0.5 μg) were used for *in vitro* transcription assays in the presence of increasing amounts of TFOs, in a buffer containing 40 mM Tris–HCl, pH 7.2, 6 mM $MgCl_2$, 2 mM spermidine, 4 mM DTT, 1 U/μl RNase inhibitor in presence of 500 μM ATP, CTP and UTP, 100 μM GTP and 0.3 μM [α-^{32}P]GTP. Transcription was initiated by addition of 25 U of phage RNA polymerase (T_7 or SP_6). After 5 min at 37°C, transcription reactions were terminated by ethanol precipitation (10 vol ethanol added to samples with 0.3 M sodium acetate and 15 μg glycogen). The transcription products were analyzed by electrophoresis on 6% polyacrylamide gels and quantifications (±10%) obtained by phosphorimager analysis. The percentages were corrected for transcript length effects taking into account that the transcripts were uniformly radiolabeled.

Cell cultures and transient expression assay

The P4-CCR5 cells were derived from HeLa cells (26) and maintained in DMEM supplemented with 10% fetal bovine serum.

P4-CCR5 cells were used for transfection of oligonucleotides and reporter vectors. Transfections were performed using the cationic activated dendrimer Superfect (Quiagen). Typically two mixtures were prepared in parallel: the plasmid containing mixture and the oligonucleotide containing one. In the plasmid mixture, 0.1 μg of (+)PPT/luc [or (+)mutPPT/luc] plasmid and 0.05 μg pRL-TK plasmid were mixed with 0.9 μl Superfect in 7.2 μl of serum-free medium, and in the oligonucleotide mixture, various amounts of oligonucleotides were mixed with 0.6 μl Superfect in 4.8 μl of serum-free medium. The two mixtures were prepared for triplicates and they were added to P4-CCR5 cells (13 750 cells per well in 96-well plate in 90 μl of serum-containing medium) at the same time; we also carried out sequential transfections separated by 24 h the oligonucleotide mixture was transfected first, and 24 h later the cells were washed before transfection of the plasmid mixture. In both cases, cells were lysed (in 30 μl of Passive Lysis Buffer, Promega) and activities of both luciferases (firefly and *Renilla*) were measured in the same cell extract using the dual-luciferase assay kit (Promega). Luciferase expressions were measured with a luminometer (Victor™-Wallac). The modulation of firefly luciferase expression by oligonucleotide treatment was quantified by evaluation of the ratio firefly/*Renilla*. Each experiment was repeated at least three times and values were presented as the mean of a triplicate (±SD) from a representative experiment.

RNA analysis

Total cellular RNA were prepared from extraction of 27 500 cells with the RNeasy Mini kit (Qiagen). Firefly and *Renilla* luciferase RNAs were subjected to competitive RT–PCR [for details from cDNA, see (27)]. Briefly two sets of two PCR primers were designed for each luciferase RNA; two competitors DNA (firefly and *Renilla*) were used and co-amplified with the RNA sample. The sequences of the primers were the following ones: for firefly, 5′ GCT GTT CTC CTC TTC CTC AT and 5′ CAG GGC GTA TCT CTT CAT AG; for *Renilla* 5′ GCG ACA TGT TGT GCC ACA TA and 5′ ATC AGG CCA TTC ATC CCA TG. Conditions for PCR were 10 min at 95°C, 35 cycles (1 min at 94°C; 30 s at 57°C, 30 s at 72°C), 10 min at 72°C.

For each luciferase, the two amplified products (from sample to competitor which are 210 and 176 bp long for firefly, and 250 and 294 bp long for *Renilla*, respectively) were separated using an 8% PAGE in TBE, and the level of RNA was quantified by Phosphorimager analysis after successive dilutions.

RESULTS

Strong and specific binding of intercalator conjugates of pyrimidine TFO/LNAs at physiological pH: defining its molecular basis

In this work we have studied the binding and biological properties of pyrimidine TFO/LNAs attached or not to a DNA intercalating agent. In the majority of experiments we used TFOs conjugated to an acridine derivative, the 2-methoxy-6-chloro-9-amino-acridine (Acr), known to intercalate in DNA, parallel to the base pairs. The acridine was attached via a linker of six carbons to the 5′-end of TFO/LNAs (Figure 1), as it was already done for other TFO chemistries, namely phosphodiester, phosphoramidates or phosphorothioates (14,15,22). LNA modifications were introduced alternatively in the sequence of (T,C)-containing TFOs, since fully modified TFO/LNAs failed to bind to double-stranded DNA (7). As a target we chose a 16 bp long oligopyrimidine·oligopurine sequence (named PPT duplex).

Stability and specificity of triplexes formed by the (T,C)-containing TFO/LNAs (Acr-16TC/LNA and 16TC/LNA) and the PPT target sequence, were first evaluated by gel shift experiments (Figure 2; Materials and Methods). TFO concentration required for 50% of complex formation (C_{50}) was estimated. Under these conditions simulating physiological ones, complex formation with the acridine-conjugated 16TC/LNA was detected in the nanomolar range [C_{50}(Acr-16TC/LNA) = 5–10 nM]. In order to estimate the influence of acridine conjugation on triplex formation, the binding of unconjugated 16TC/LNA to the PPT duplex was assessed under the same conditions, and 50% triplex formation was seen at 100 nM concentration. Quantifications of the retarded band, reflecting complex formation, was reported for various TFO concentrations (Figure 2B). In the presence of Acr-16TC/LNA, 90% of complex was formed at a concentration as low as 25 nM, whereas 250 nM of unconjugated 16TC/

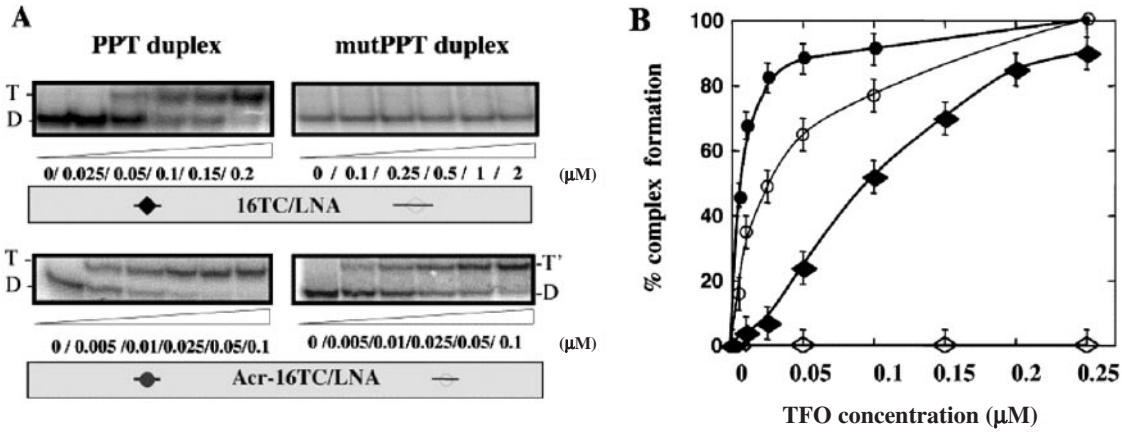

Figure 2. Triplex formation with (T,C)-containing TFO/LNAs: gel shift assays. **(A)** Increasing concentrations of 16TC/LNA or Acr-16TC/LNA were incubated in 150 mM sodium chloride, 50 mM HEPES pH 7.2, 1 mM $MgCl_2$ and 0.5 mM spermine, either with PPT (left) or mutPPT (right) duplex. The samples were analysed by electrophoresis in 15% non-denaturing polyacrylamide gel (50 mM HEPES, pH 7.2, 1 mM $MgCl_2$) at 37°C. D: duplex; (T, T′): triplex. **(B)** Quantification of retarded band reflecting complex formation between 16TC/LNA (filled or open diamonds) or Acr-16TC/LNA (filled or open circles) and PPT or mutPPT duplex (filled or open symbols, respectively). C_{50} values corresponding to TFO concentrations for 50% triplex formation were estimated from these gel shift quantifications.

LNA was required for equivalent binding. It is noticeable that under these conditions the isosequential Acr-16TC/po was unable to form a complex with the PPT target up to 10 μM, consistent with high LNA-induced stabilization, as already described for other LNA-modified TFOs (8).

In order to assess the specificity of duplex recognition by the 16TC/LNA, conjugated or not to the acridine unit, we compared their binding to the PPT duplex target and to the mutPPT duplex containing two mutations in the triplex site (5′ AAAAGAAAA**A**GG**A**GGA-3′, mutations in bold). For the unconjugated 16TC/LNA, no binding was detected up to 2 μM (at this concentration the complex was completely formed on PPT duplex). For the Acr-16TC/LNA, a 5-fold increase in C_{50} was obtained compared to the wild-type sequence [C_{50} (Acr-16TC/LNA; mutPPT) = 25 nM]. These data on binding selectivity [for 16TC/LNA, C_{50}(mutPPT)/C_{50}(PPT) > 20 and for Acr-16TC/LNA, C_{50}(mutPPT)/C_{50}(PPT) = 5] must be commented taking into account the facts that: (i) nine contiguous triplets could theoretically be formed with the A_4GA_4 sequence on both of the two targets (PPT and mutPPT); (ii) in our experimental conditions (neutral pH) the binding was mainly driven by the T-rich part of the 16TC sequence (5′-TTTCTTTT; as it will be shown later); (iii) this T-rich part is attached to acridine in Acr-16TC/LNA. Thus in the Acr-16TC/LNA, acridine intercalation should stabilize the formation of the nine base triplets to the mutPPT duplex and prevent dissociation during gel analysis when compared to the 16TC/LNA. Indeed with the mutPPT duplex the migration of the retarded band (T) was reduced compared to that observed with the PPT duplex (T), consistent with a less compact structure that might correspond to a partial binding of the Acr-16TC/LNA.

To further quantify the binding to DNA of pyrimidine TFO/LNAs and the influence of acridine conjugation, UV absorption melting experiments were carried out (Table 1). As expected, the presence of the intercalating agent at the 5′-end of the 16TC/LNA strongly increases the triplex-forming ability of the oligomers compared to the unconjugated 16TC/LNA. Thus a ~10°C increase in the melting temperature was observed compared to the corresponding pyrimidine sequence 16TC/LNA [T_m(Acr-16TC/LNA) = 41°C and T_m(16TC/LNA) ~29.5°C]. As expected the presence of LNA modifications results in a strong increase in T_m compared to the isosequential phosphodiester TFOs conjugated or not to acridine (Acr-16TC/po, 16/TC/po). These data on acridine-induced stabilization of TFO/LNAs are consistent with those obtained with other TFO chemistries.

The binding specificity of the Acr-16TC/LNA was evaluated, using the mutPPT duplex as a target like in gel shift assays. We showed that Acr-16TC/LNA could discriminate between the wild-type and the mutated target with a large

Table 1. Melting temperatures (T_m values) of the different (T,C)-containing TFOs with the PPT or mutPPT target duplex (indicated in brackets) in different buffer conditions

TFO	pH	Buffer	T_m(°C) Target: PPTduplex (mutPPT duplex)
Acr-16TC/LNA	7.0	L	41 (31)
16TC/LNA	7.0	L	29.5[a](n.d)
Acr-16TC/LNA	7.0	H	n.d.
16TC/LNA	7.0	H	37 (34)
9TC/LNA	7.0	H	37 (37)
16TC/LNA	6.5	H	47 (38)
9TC/LNA	6.5	H	42 (42)
16TC/po	6.5	H	10[b]
16TC/LNA	6.0	H	56
9TC/LNA	6.0	H	46 (45)
Acr-16TC/po	6.0	H	35 (30)
16TC/po	6.0	H	18

The data were obtained in a buffer containing 10 mM cacodylate, 150 mM sodium chloride, 10 mM $MgCl_2$ (Buffer H) or in 10 mM cacodylate, 100 mM sodium chloride (Buffer L). Strand concentrations: 1 μM PPT duplex and 1.5 μM TFO. Specific conditions are indicated. Estimated errors in T_m (±) 0.5°C, or (±) 1.5°C for cases indicated with ([a] and [b]), which correspond to a triplex transition with a hysteresis phenomenon between cooling and heating profiles (Figure S1) or with a melting profile lacking a complete base line at low temperatures, respectively. (n.d.): not determined, either because the triplex and duplex transitions were superimposed or the triplex transition presented a weak hyperchromic change and a hysteresis profile.

Table 2. Kinetics of triplexes formed with different TFO/LNAs: kinetic rate constants k_{off} and k_{on} and the corresponding calculated equilibrium constants $K_d = (k_{off}/k_{on})$

TFO	T(°C)	pH	$k_{on}(M^{-1}s^{-1})$	$k_{on}(s^{-1})$	$\tau(s) = \ln 2/k_{off}$	$K_d = k_{off}/k_{on}$ (M)
Acr-16TC/LNA	37	7.0	$3.3 \times 10^3 (r^2 = 0.98)$	2.5×10^{-5} ($\pm 7 \times 10^{-6}$)	2.8×10^5	8.4×10^{-9}
16TC/LNA	37	7.0	0.9×10^3 ($r^2 = 0.99$)	1.5×10^{-3} ($\pm 2.5 \times 10^{-4}$)	4.6×10^2	1.7×10^{-6}
9TC/LNA	37	7.0	2.0×10^3 ($r^2 = 0.985$)	1.5×10^{-3} ($\pm 4 \times 10^{-4}$)	4.6×10^2	7.2×10^{-7}
16TC/LNA	37	6.5	1.3×10^3 ($r^2 = 0.99$)	1.6×10^{-4} ($\pm 2 \times 10^{-6}$)	4.6×10^3	1.2×10^{-7}
9TC/LNA	37	6.5	2.5×10^3 ($r^2 = 0.98$)	1.1×10^{-3} ($\pm 4 \times 10^{-5}$)	6.3×10^2	4.4×10^{-7}

The data were obtained in a buffer containing 10 mM cacodylate, 150 mM sodium chloride, 10 mM $MgCl_2$, P20 0.0005% (Buffer H). Specific conditions are indicated. The half-life (τ) of triplex was also reported. Correlation coefficients (r^2) are reported.

decrease in T_m [ΔT_m (PPT-mutPPT) = 10°C in Buffer L; Table 1]. This was also the case for the 16TC/LNA.

These results obtained with Acr-16TC/LNAs in two different experimental settings show the formation of a highly stable complex with the Acr-16TC/LNA under conditions closely mimicking physiological ones, and demonstrate a strong increase in thermal stability induced by conjugation of an intercalator still allowing specific binding of acridine-conjugated TFO/LNA to the PPT duplex target.

To investigate the origin of the high stability of triplexes formed with TFO/LNA-intercalator conjugates, we performed kinetic analyses using SPR experiments with the Acr-16TC/LNA and the 16TC/LNA (Table 2).

Compared to the unconjugated 16TC/LNA, triplex formation with the conjugate exhibited a slightly faster (~3-fold) association rate and a much slower dissociation (~50-fold decrease in k_{off}). These kinetic data demonstrate that the significant stabilization observed for triplexes formed with the TFO/LNA-intercalator conjugates [K_d (37°C; Acr-16TC/LNA) ~8.4 nM; K_d (37°C; 16TC/LNA) = 1.7 μM; Figure 3] are mainly due to a longer lifetime [$\tau = (\ln 2/k_{off})$ in the range of ~10 h at 37°C compared to ~7.5 min for the unconjugated TFO/LNA] and to a lesser extent, to a faster association (3-fold increase compared to the unconjugated 16TC/LNA).

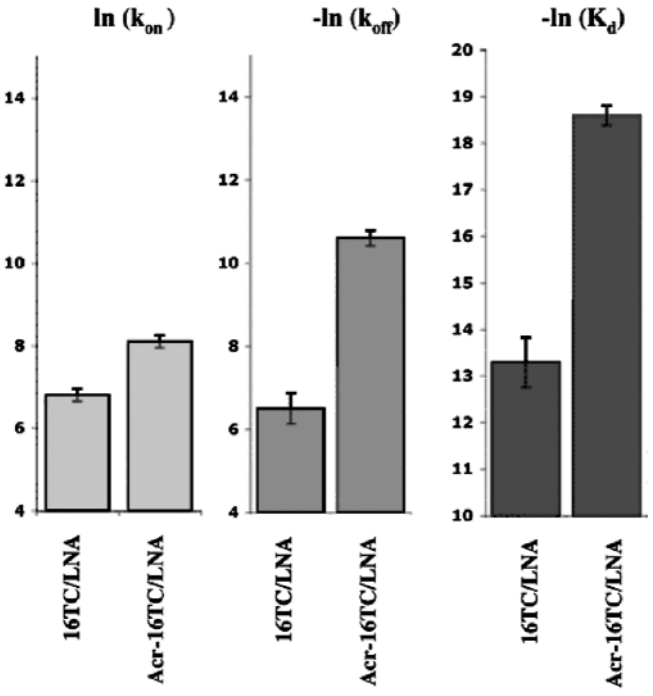

Figure 3. SPR experiments. Values of $\ln(k_{on})$, $-\ln(k_{off})$ (association and dissociation rate constants) and $-\ln(K_d)$ (equilibrium dissociation constant) for the different triplexes formed with (T,C)-containing TFO/LNAs. These values were obtained at 37°C in a buffer containing 10 mM cacodylate, 150 mM sodium chloride, 10 mM $MgCl_2$, P20 0.0005%.

pH-dependence of pyrimidine TFO/LNA binding

The pH-induced effects on triplexes formed with pyrimidine TFO/LNAs were studied using UV absorption melting (Figure 4, Table 1) and SPR experiments (Table 2).

Two different pyrimidine TFO/LNAs were studied (16TC/LNA and 9TC/LNA), all composed of alternating LNA and DNA nucleotides along the sequence, with all cytosines being methylated (Figure 1). The shorter TFO (9TC/LNA) is a truncated version of the 16TC/LNA, lacking the C-rich sequence (CCCCCCT-3′) and is used to evaluate, as a function of the pH value, the binding of the C-rich part of the 16TC sequences by comparison with the 16TC/LNA.

We first examined the thermal stability of triplexes formed with the different (T,C)-containing TFO/LNAs at different pH values and compared to results obtained with phosphodiester TFOs. Since Acr-16TC/LNA exhibited high T_m value at pH value as high as 7 it was excluded from the study, but the pH-dependence of triplex formation is likely governed by the oligonucleotide part of the conjugate and results obtained with the 16TC/LNA may be valid also for the Acr-16TC/LNA.

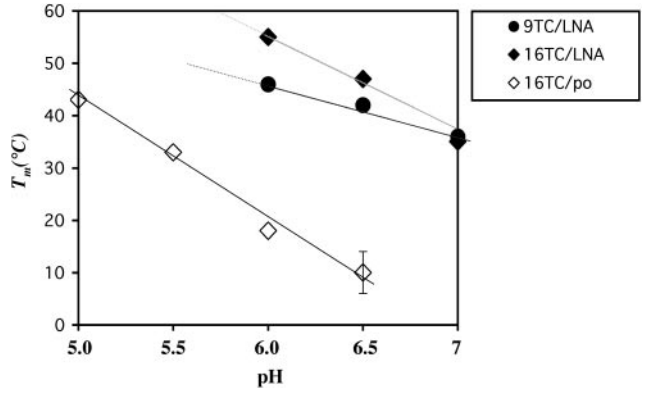

Figure 4. pH variations of melting temperatures [T_m (°C)] of the different (T,C)-containing TFOs with the PPT duplex target. Melting temperatures were obtained in a buffer containing 10 mM cacodylate, 150 mM sodium chloride and 10 mM $MgCl_2$.

All the TFOs showed a decrease in T_m when the pH increased, as expected for C-containing TFOs, ascribed to the loss of cytosine protonation. As described in Figure 4, the pH-dependence seemed to be equivalent for triplexes formed with 16TC/LNAs compared to the ones formed with the unmodified 16TC/po [as measured by the slope of the graph $T_m = f(pH)$]. Noteworthy no binding was detected ($T_m < 10°C$) with the 16TC/po above pH 6.5 whereas the 16TC/LNA was strongly bound at pH 7 ($T_m = 47°C$).

To obtain information concerning the binding of the 3′ C-rich portion (CCCCCCT-3′) in the 16TC sequence the stabilities of different triplexes were measured. First the binding to the PPT duplex of the 16TC/LNA was compared with that of the 9TC/LNA (T_m values in Table 1). The deletion of the six contiguous cytosines in the 9TC sequence induced a decrease in triplex stability below pH 7, this decrease being stronger at lower pH values [ΔT_m(16TC/LNA-9TC/LNA) = 1, 5 and 9°C at pH 7, 6.5 and 6, respectively], consistent with the different cytosine content of the TFOs (one in 9TC and seven in 16TC). Second, we evaluated the binding of the 16TC/LNA to the mutated PPT duplex containing the two mutations (**AGGAG**GA-3′, mutations in bold) in the region recognized by the 3′-end of the 16TC (CCCCCCT-3′). The selective recognition of the two targets by the 16TC/LNA increased when pH decreased [ΔT_m(PPT-mutPPT; 16TC/LNA) = 3 and 9°C at pH 7 and 6.5, respectively].

This set of results are consistent with the fact that at neutral pH, triplex stability with the 16TC/LNA was mainly driven by the binding of the 5′ T-rich portion (5′-tTtTcTtTt) that corresponds to the 9TC/LNA sequence. The binding of the 3′ C-rich portion increased as the pH was decreased, favoring the protonation of the cytosine segment.

To further understand the pH-dependence of triplex formation with pyrimidine TFO/LNAs. The 16TC/LNA and 9TC/LNA were studied at pH 7 and 6.5 (Table 2). Changes in pH values from 6.5 to 7 affected the stability of the triplex formed with 16TC/LNA (14-fold increase in K_d/+ 0.5 unit of pH) more than that of the one formed with 9TC/LNA (1.6-fold increase in K_d/+ 0.5 unit of pH), supporting the results obtained by UV T_m measurements and consistent with the different cytosine composition, position and distribution (one internal in 9TC and, six terminal and adjacent in 16TC) (28). From a kinetic point of view, K_d variations as the pH was increased from 6.5 to 7, appeared to be mainly driven by k_{off}, leading to faster dissociations. The association was marginally affected by pH variation for both 9TC/LNA and 16TC/LNA. However, whatever the pH value (7 or 6.5), the 9TC/LNA did associate significantly faster (~2-fold) compared to the 16TC/LNA, as expected for a shorter TFO.

Pyrimidine TFO/LNAs are efficient to interfere with DNA acting proteins *in vitro*

To further characterize the DNA binding of (T,C)-containing TFO/LNA, we evaluated the capacity of the corresponding triplexes to interfere with DNA acting proteins, i.e. either a restriction enzyme or an RNA polymerase.

First we exploited the fact that a Dra I cleavage site (TTT↓**AAA**) is present at the 5′ side of the PPT oligopurine strand and overlaps the PPT target on 3 bp. When triplex formation occurred, Dra I cleavage was impaired only on the site overlapping the PPT sequence. The TFO concentrations for 50% of Dra I cleavage inhibition (IC_{50}) were determined (Supplementary Figure S3): ~250 nM for the 16TC/LNA and ~25 nM for the Acr-16TC/LNA, with a complete inhibition at 100–200 nM. Under the same conditions the isosequential phosphodiester TFOs (16TC/po and Acr-16TC/po) did not inhibit cleavage at 37°C up to a concentration of 10 μM.

Second, the pyrimidine TFO/LNAs were evaluated for their ability to interfere *in vitro* with an RNA polymerase moving along the DNA. To address this point, a plasmid containing the T_7 polymerase promoter upstream the PPT site was used as template for transcription assays (Figure 5). As shown on the gel, templates harboring some of the triple-helical complexes directed the synthesis of a truncated transcript of ~330 nt. Thus Acr-16TC/LNA was able to inhibit RNA synthesis more efficiently than the unconjugated 16TC/LNA: ~50% of truncated transcripts were observed at 0.05 μM of Acr-16TC/LNA compared to 1 μM of 16TC/LNA. Under these transcription conditions the phosphodiester TFOs (16TC/po and Acr-16TC/po) were unable to inhibit transcription (upto 10 μM).

The specificity of transcription inhibition was established according to several experiments. First, no effect was observed with another pyrimidine LNA oligonucleotide (16py(1)/LNA, sequence in Figure 1). Second, to demonstrate a triplex-mediated inhibition of transcription, the site of transcription arrest obtained in the presence of TFO, was compared to a run-off transcription product using the template plasmid digested by Dra I; this restriction enzyme cleaves exactly at the 5′ boundary of the PPT oligopurine sequence (lane M, Figure 5B).

Finally, SP_6 RNA polymerase was used to initiate transcription in the opposite direction as compared to the T_7 RNA polymerase (Figure 5A). SP_6 transcription in the presence of pyrimidine TFO/LNAs also produced a truncated product that corresponded to an arrest of RNA synthesis at the PPT site, localized by the Dra I marker as described above (data not shown), and the TFO-acridine conjugate was still more effective than the unconjugated TFO at arresting elongating SP_6 RNA polymerase. These results support a physical blockage of the RNA polymerase by the TFO/LNAs, whatever the triplex side encountered by the polymerase, the 5′ side of the PPT oligopurine sequence corresponding to the acridine intercalation site at the duplex–triplex junction (during T_7 transcription) or the opposite one (during SP_6 transcription).

These data on two different DNA-associated biological activities of pyrimidine TFO/LNA were consistent with physico-chemical data from UV spectroscopy and gel shift analyses described above: strong and still specific binding to PPT DNA target, increase in stability induced by intercalator conjugation (as measured here by 10/20-fold decrease in inhibitory concentrations) and finally, higher stability of triplexes formed with TFO/LNA compared to TFO/po.

Triplex-based activity in cells mediated by pyrimidine TFO/LNAs at submicromolar concentrations

To date, pyrimidine TFO/LNAs have not been tested in cells. The *in vitro* properties described above, especially those of the conjugated TFO, Acr-16TC/LNA, would seem consistent with activity in cell-based assays. Cellular activities of pyrimidine

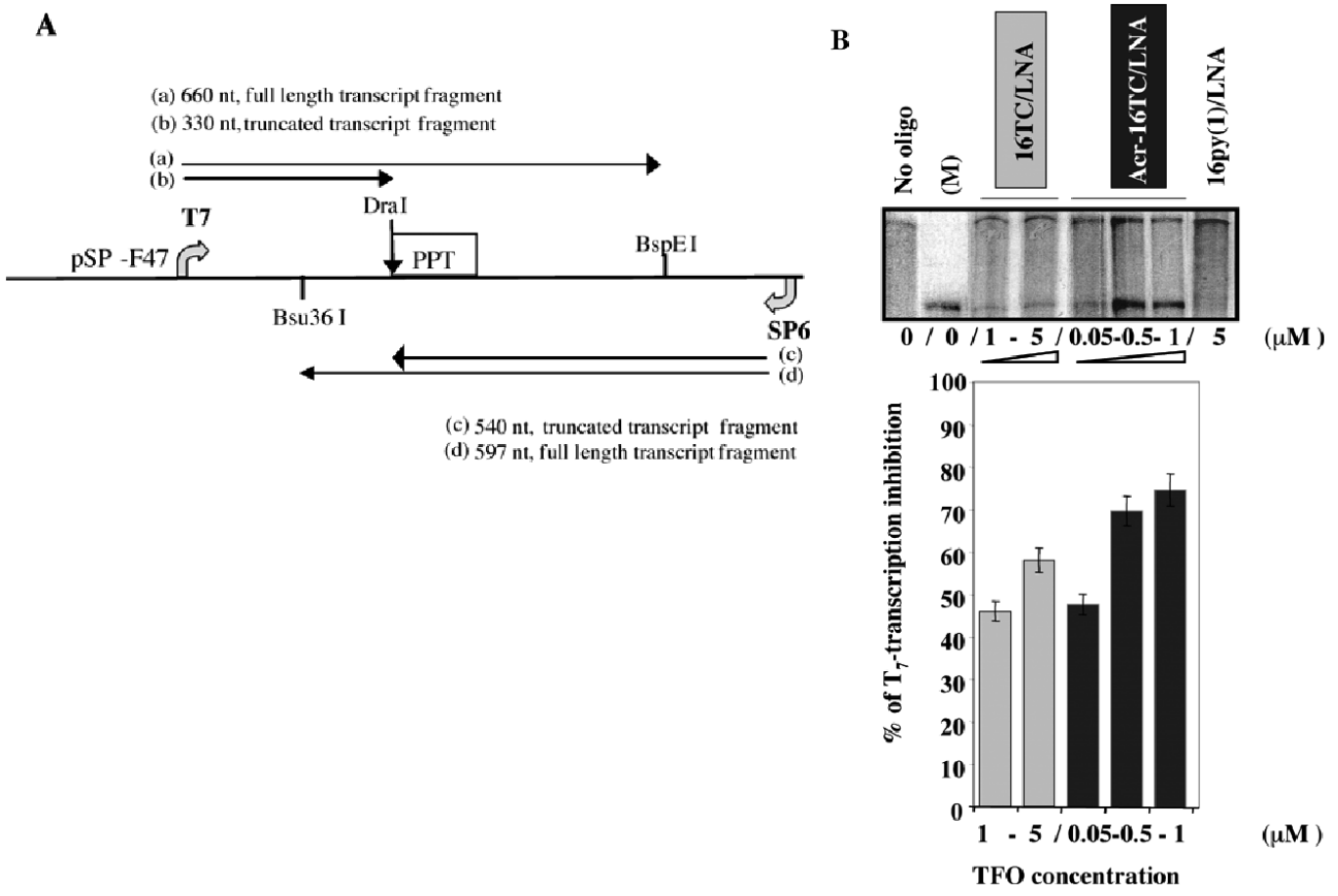

Figure 5. *In vitro* arrest of RNA synthesis by (T,C)-containing TFO/LNAs. **(A)** Description of the transcription system. The pSP-F47 plasmid contains the PPT target between two bacteriophage promoters (T_7 and SP_6). Full-length transcripts (660 or 597 nt long, respectively.) correspond to transcription of the BspE I or Bsu36 I (resp.) linearized pSP-F47 plasmid; the PPT sequence is positioned (330 or 540 nt, respectively), downstream of the transcription initiation site; truncated transcripts are compared to transcripts of Dra I-linearized pSP-F47 plasmid, used as size markers (Dra I RNA marker; lane (M) in Figure 5B). **(B)** *In vitro* transcription assay. BspE I-linearized plasmid was incubated in the absence or in the presence of different concentrations of TFO/LNAs and used as template for T_7 transcription. The transcription products (full-length and truncated) were analysed by electrophoresis on a 6% polyacrylamide sequencing gel. Lane (M): Dra I RNA marker. Quantification of transcription inhibition measured by the percentage of truncated transcripts (corrected by transcript lengths) is reported below the gel.

TFO/LNAs were estimated in a transient expression system that was designed for quantitative and fast evaluation of molecules targeted against the oligopyrimidine•oligopurine PPT sequence and for demonstration of a triplex-based mechanism. Indeed two different DNA templates [(+)PPT/luc and (+)mutPPT/luc plasmids] coding for the firefly luciferase and containing the wild-type PPT sequence or the mutated sequence (mutPPT with two mutations, Figure 1) were used. The PPT or the mutPPT sequence was located in the transcribed but untranslated region of luc gene (Figure 6A). HeLa cells were transiently transfected with the (+)PPT/luc plasmid [or the (+)mutPPT/luc plasmid] together with the pRL-TK plasmid (expressing *Renilla* luciferase and used for correction of transfection efficiency) and with various TFOs. Two transfection mixtures were prepared for plasmids and TFO, respectively, in order to prevent direct interaction between TFO and DNA template before transfection; the two mixtures were added to cell cultures simultaneously. The modulation of firefly luciferase expression and messenger RNA (mRNA) levels induced by TFO treatment was evaluated 24 h after treatment. The activities of different pyrimidine TFO/LNAs (sequences in Figure 1) were determined and results are reported in Figure 6.

Acr-16TC/LNA did induce an inhibition of firefly luciferase expression, with 50% inhibition at ~50–100 nM. To establish triplex involvement in the observed inhibition several criteria were examined. First, a control LNA oligonucleotide-acridine conjugate was used, presenting the same base composition as the 16TC/LNA and with an acridine unit at its 5′-end (Acr-16py(2)/LNA): after treatment with this oligonucleotide no decrease in luciferase activity was detected in conditions where the specific Acr-16TC/LNA-induced 75% luciferase inhibition. Second the (+)mutPPT/luc plasmid was treated with the Acr-16TC/LNA: the presence of two mutations in the PPT target sequence abolished the inhibitory effect of Acr-16TC/LNA. Third firefly luciferase mRNAs were quantified: in the presence of Acr-16TC/LNA a reduction of luciferase RNA levels did occur (Figure 6C), together with the decrease in luciferase protein. This excluded that the TFO/LNA could act by binding to the oligopurine sequence present on the mRNA produced from the (+)PPT/luc DNA. Indeed the used TFO/LNAs (with alternating LNA and DNA along the

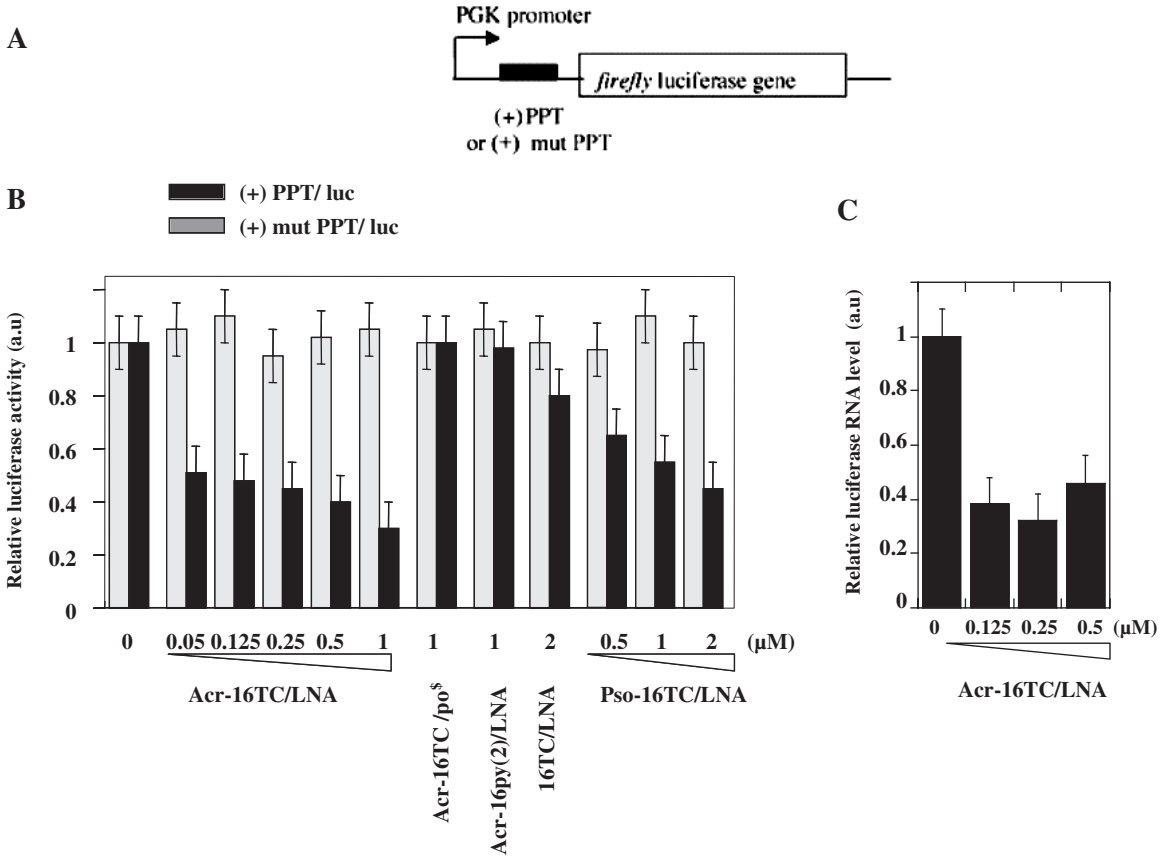

Figure 6. Cellular activity of (T,C)-containing TFO/LNAs: inhibition of transcription elongation. **(A)** Experimental design. Schematic representation of the (+)PPT/luc or (+)mutPPT/luc plasmids. These plasmids allow expression of the firefly luciferase reporter gene (luc) (Materials and Methods). The PPT (or the mutPPT 5′, AAAAGAAAAAGGAGGA-3′, two mutations in bold) sequence was inserted just upstream the luc gene. (**B**) The expression vector, (+)PPT/luc or (+)mutPPT/luc plasmid, was introduced with the pRL-TK plasmid, in the presence or absence of (T,C)-containing TFO/LNAs. Plasmids and TFOs were introduced independently using two transfection mixtures that were added to the cells at the same time. Cell extracts were analysed for firefly and *Renilla* luciferases activities, 24 h after transfection by a cationic dendrimer (Superfect). Normalized firefly/*Renilla* luminescence intensity ratios are reported for different TFO/LNA concentrations. Data are derived from at least four experiments. Acr-16TC/po$^{\$}$ = Acr-16TC/po, 3′-modified by incorporation of a propylamine group. (**C**) Ratio of (Firefly/*Renilla*) RNA levels was deduced from competitive RT–PCR (Materials and Methods): decrease of RNA level was compared with that obtained for transfection of (+)PPT/luc and RL-TK plasmids in absence of TFO/LNAs.

sequence) were unable to induce RNase H activation *in vitro* when bound to the PPT RNA sequence (data not shown), as expected from previous work (29). This set of data demonstrated that the TFO-induced activity was caused by complex formation on the PPT sequence, leading to transcriptional inhibition at the DNA level. Noteworthy triplex formation likely occured intracellularly in our experimental conditions. Indeed, the same level of luciferase inhibition was induced by the Acr-16TC/LNA when the TFO and DNA template were introduced within the cells simultaneously (as previously described) or sequentially (first, TFO and 24 h later, DNA; Materials and Methods; Supplementary Figure S4).

The efficacy of triplex-induced inhibition was studied by using various pyrimidine TFOs. The unconjugated 16TC/LNA was much less active than the Acr-16TC/LNA, with >20-fold increase in the IC_{50} (~30% inhibition at 2 μM); equivalent activity was obtained with 16TC/LNA and 16TC/LNA (differing by the presence of methylated or unmodified DNA cytosines), consistent with the thermal stability data. To evaluate the activity of another TFO-intercalator conjugate commonly used in triplex-based applications, the 5′-end of the 16TC/LNA was linked to a psoralen derivative (Pso-16TC/LNA). As with the acridine, the psoralen moiety should intercalate at the duplex–triplex junction and thus increase the stability of the non-covalent triplex in the absence of photoactivation, as already described for other TFO chemistries (18,30). The psoralen-conjugated TFO was more active in cells than the unconjugated 16TC/LNA and significantly less efficient than the isosequential acridine conjugate (50% inhibition at 1 μM for the Pso-16TC/LNA compared to >2 μM for the 16TC/LNA and 50–100 nM for the Acr-16TC/LNA). For all tested TFOs triplex involvement was supported by the absence of luciferase inhibition in the (+)mutPPT system. Finally, under the same conditions, no activity was observed for the phosphodiester Acr-16TC/po.

These data support the high potency of pyrimidine TFO/LNAs attached to DNA intercalating agents, in contrast to phophodiester pyrimidine TFOs, for triplex-based applications in cells.

DISCUSSION

In the present work we have characterized the binding properties and cellular activities of triplexes formed with

pyrimidine TFO/LNAs; we have compared TFO/LNAs attached or not to an intercalating agent (Acr-16TC/LNA and 16TC/LNA, respectively) with the aim to determine the specific influence of intercalator conjugation in the context of pyrimidine TFO/LNAs. We showed that the TFO/LNAs are reliably active intracellularly at levels that might permit experimentation on a variety of interesting issues and we have attempted to understand the biophysical parameters that underlie TFO/LNA bioactivity.

Our *in vitro* data (obtained at 37°C and neutral pH) showed a strong DNA binding of Acr-16TC/LNA with a dissociation equilibrium constant (K_d) of ~10 nM, 200-fold lower than for the unconjugated 16TC/LNA. Such high affinity is not detrimental for specificity, since binding strongly decreases when mutations are present in the DNA target. These data concerning acridine-induced triplex stabilization extend the results obtained with other TFO chemistries to TFO/LNAs; noteworthy the use of LNA modifications is associated with tight binding of pyrimidine and C-rich TFOs (16TC sequence) in conditions simulating physiological ones. Here we have proceeded towards an understanding of the origins of triplex stabilization observed with the conjugated compared to the unconjugated TFO. To address this question we performed kinetic analyses. We demonstrated that triplex stabilization induced by acridine conjugation was mainly due to a decrease in the dissociation rate constant, with residence time in the range of 10 h; the association rates were also slightly more favorable, with a 3-fold increase. The origins of the increased association rate might be attributed to protonation of the aminoacridine unit inducing favorable electrostatic interactions. The decreased dissociation rate is consistent with intercalation of the acridine moiety at the duplex–triplex junction, that is a 5′-YpR-3′ sequence known to be particularly appropriate.

This high triplex stability observed for the studied pyrimidine TFO/LNAs translates into biological activities. We evaluated the *in vitro* and cellular activities of TFO/LNAs using experimental systems designed to demonstrate quantitatively and rapidly a triplex-based mechanism. Their capacity to interfere with transcription elongation was estimated. We could demonstrate the triplex involvement in transcription arrest, both *in vitro* and in cells: *in vitro* RNA synthesis was halted at the triplex site where the TFO was formed; in cells, the transcription of the target gene was inhibited whereas the expression of the gene containing a mutated version of the target sequence (mutPPT DNA with two mutations) was not affected. Our data also showed that both LNA modifications and intercalator attachment did increase TFO activity without affecting its sequence-specificity, consistent with binding data obtained *in vitro*. In addition to the acridine derivative we tested another commonly used intercalating agent, the psoralen; its mode of intercalation is close to that of acridine, with binding parallel to the base pairs. Psoralen conjugation (in Pso-16TC/LNA) also induced an increase in activity but to a lesser extent compared to the acridine [IC_{50}(Pso-16TC/LNA) ~1 μM compared to IC_{50}(Acr-16TC/LNA) ~0.1 μM]. Such difference might be due to the formation of a slightly less stable triplex (data not shown) and more likely to different intracellular transfer of the two conjugates. Indeed conjugation of acridine was demonstrated to improve delivery when the conjugate was transfected with cationic reagents (31).

Concerning efficiency, the activity of acridine-conjugated 16TC/LNA was observed at relatively low TFO concentrations (IC_{50}~0.1 μM). Generally pyrimidine TFOs and especially C-rich sequences are described to be poorly active in cells and G-containing TFOs [(T,G)- and (A,G)-motifs] have therefore mainly been used [for a review in (2)]. The latter have also been attached to intercalating agents (psoralen, daunomycin, acridine) and have been used successfully either to induce targeted mutagenesis or to inhibit transcription (15,17,18). In all cases they have exhibited inhibitory activity in the micromolar range (~0.5–1 μM, 24 h after treatment) when administrated with cationic agents. To our knowledge, cellular activities of non-covalent pyrimidine triplexes were not previously reported however, in two systems (19,32) pyrimidine psoralen-linked TFOs were described to be active when photoactivation was performed to induce a targeted DNA cross-link. In one case, a 15mer phosphodiester TFO directed against the IL2-Rα promoter was able to partially prevent transcription factor binding and then to inhibit transcription initiation, when preincubated *in vitro* with the target plasmid and electroporated (at 20 μM in the electroporation mixture). In the second case, a T-rich TFO containing 2′-modified sugars directed against the HPRT gene was able to cross-link the target locus (at 5 μM in the electroporation mixture) and mutations were induced at the triplex site, due to triplex processing by the repair machinery. Of course comparison of TFO efficiency in different experimental settings (TFO sequence, target gene, cell type, delivery methods) for different types of activities (inhibition of transcription (initiation or elongation) or induction of mutations) is difficult, but high efficiency of Acr-16TC/LNA was observed here, supporting the potential of pyrimidine TFO/LNA for triplex-based applications in cells with efficient targeting of chromosomally located genes under conditions where TFO/LNAs were highly active, the parent phosphodiester oligonucleotides did not exhibit any inhibitory effect. Noteworthy our experimental system is quite unfavorable: indeed, the target sequence was relatively short (16 bp) including six contiguous (CG bp), and the cellular activity to inhibit was transcription elongation, known to be difficult to arrest. TFO/LNAs might likely be active at still lower concentrations in another context when interference with other biological activities is envisioned.

Finally the use of pyrimidine TFOs versus G-containing ones presents some advantages, e.g. a lower tendency to self-associate under physiological conditions and a lower ability to bind cellular proteins, a phenomenon competing with triplex formation and potentially leading to unexpected cellular effects, and the potency to target all oligopyrimidine·oligopurine sequences, due to a perfect isomorphism between the T·AxT and C·GxC+ base triplets. However the major disadvantage is their pH-dependent binding to DNA which generally makes the corresponding triplex unstable at neutral pH. In this work we explored the pH-dependence of triplexes formed with pyrimidine TFO/LNAs. Kinetically the major effect did concern the dissociation process, as already reported for non-modified triplexes (24): a pH increase was associated with a faster dissociation. However with Acr-16TC/LNA a stable triplex was still formed at neutral pH under conditions closely mimicking physiological ones and cellular activity was realised. It is likely that pyrimidine TFO/LNA

attached to other intercalators with the same binding mode will have similar properties, as illustrated here with the TFO/LNA-psoralen conjugate.

Targeted gene knock-down is possible with different powerful techniques, including antisense and siRNA approaches. However among oligonucleotide-based technologies, TFOs offer unique potential since, as DNA binding molecules that recognize specific sequences, they can be used to understand DNA-occuring processes and the associated biological functions. In this context TFO can also be useful as DNA recognition elements for the positioning of DNA interacting or reactive compounds, such as anticancer drugs (33), based on chemical conjugation of these agents with TFO (34,35). Manipulation of chromatin structure is another promising application of TFOs (36,37). These two latter aspects have been successfully explored *in vitro*. For further triplex-based cellular experiments it is still necessary to identify novel TFO chemistries, associated with increased activities, that are easy to synthetize and compatible with conjugation synthesis. The LNA-modified pyrimidine oligonucleotides described here fulfill these criteria. Our work is the initial step for their use in future developments of innovative antigene applications.

SUPPLEMENTARY MATERIAL

Supplementary Material is available at NAR Online.

ACKNOWLEDGEMENTS

We thank Patrizia Alberti and Fabio Cannata for technical assistance and Thérèse Garestier-Hélène for careful reading of the manuscript. This work was supported by grants from La Ligue Nationale Contre le Cancer. E.B. is supported by the French Ministery for Research. The Danish National Research Foundation is acknowledged for financial support. Funding to pay the Open Access publication charges for this article was provided by INSERM.

Conflict of interest statement. None declared.

REFERENCES

1. Faria,M. and Giovannangeli,C. (2001) Triplex-forming molecules: from concepts to applications. *J. Gene. Med.*, **3**, 299–310.
2. Besch,R., Giovannangeli,C. and Degitz,K. (2004) Triplex-forming oligonucleotides—sequence-specific DNA ligands as tools for gene inhibition and for modulation of DNA-associated functions. *Current Drug Targets*, **5**, 691–703.
3. Kuan,J.Y. and Glazer,P.M. (2004) Targeted gene modification using triplex-forming oligonucleotides. *Methods Mol. Biol.*, **262**, 173–194.
4. Koshkin,A., Rajwanshi,V.K. and Wengel,J. (1998) Novel convenient syntheses of LNA [2.2.1] bicyclo nucleosides. *Tetrahedron Lett.*, **39**, 4381–4384.
5. Obika,S., Nanbu,D., Hari,Y., Andoh,J., Morio,K., Doi,T. and Imanishi,T. (1998) Stability and structural features of the duplexes containing nucleoside analogues with a fixed N-type conformation, 2′-O,4′-C-methyleneribonucleosides. *Tetrahedron Lett.*, **39**, 5401–5404.
6. Obika,S., Uneda,T., Sugimoto,T., Nanbu,D., Minami,T., Doi,T. and Imanishi,T. (2001) 2′-O,4′-C-Methylene bridged nucleic acid (2′,4′-BNA): synthesis and triplex-forming properties. *Bioorg. Med. Chem.*, **9**, 1001–1011.
7. Koizumi,M., Morita,K., Daigo,M., Tsutsumi,S., Abe,K., Obika,S. and Imanishi,T. (2003) Triplex formation with 2′-O,4′-C-ethylene-bridged nucleic acids (ENA) having C3′-endo conformation at physiological pH. *Nucleic Acids Res.*, **31**, 3267–3273.
8. Torigoe,H., Hari,Y., Sekiguchi,M., Obika,S. and Imanishi,T. (2001) 2′-O,4′-C-methylene bridged nucleic acid modification promotes pyrimidine motif triplex DNA formation at physiological pH: thermodynamic and kinetic studies. *J. Biol. Chem.*, **276**, 2354–2360.
9. Hertoghs,K.M., Ellis,J.H. and Catchpole,I.R. (2003) Use of locked nucleic acid oligonucleotides to add functionality to plasmid DNA. *Nucleic Acids Res.*, **31**, 5817–5830.
10. Fluiter,K., ten Asbroek,A.L., de Wissel,M.B., Jakobs,M.E., Wissenbach,M., Olsson,H., Olsen,O., Oerum,H. and Baas,F. (2003) *In vivo* tumor growth inhibition and biodistribution studies of locked nucleic acid (LNA) antisense oligonucleotides. *Nucleic Acids Res.*, **31**, 953–962.
11. Jepsen,J.S. and Wengel,J. (2004) LNA-antisense rivals siRNA for gene silencing. *Curr. Opin. Drug Discov. Devel.*, **7**, 188–194.
12. Giovannangeli,C., Sun,J.-S. and Helene,C. (1996) Nucleic acids: supramolecular structures and rational design of sequence-specific ligands. In Murakami,Y. (ed.), *Comprehensive supramolecular chemistry*. Pergamon, Vol. 4, pp. 177–192.
13. Sun,J.S., Francois,J.C., Montenay-Garestier,T., Saison-Behmoaras,T., Roig,V., Thuong,N.T. and Helene,C. (1989) Sequence-specific intercalating agents: intercalation at specific sequences on duplex DNA via major groove recognition by oligonucleotide-intercalator conjugates. *Proc. Natl Acad. Sci. USA*, **86**, 9198–9202.
14. Lacoste,J., Francois,J.C. and Helene,C. (1997) Triple helix formation with purine-rich phosphorothioate-containing oligonucleotides covalently linked to an acridine derivative. *Nucleic Acids Res.*, **25**, 1991–1998.
15. Faria,M., Wood,C.D., Perrouault,L., Nelson,J.S., Winter,A., White,M.R., Helene,C. and Giovannangeli,C. (2000) Targeted inhibition of transcription elongation in cells mediated by triplex-forming oligonucleotides. *Proc. Natl Acad. Sci. USA*, **97**, 3862–3867.
16. Chomilier,J., Sun,J.S., Collier,D.A., Garestier,T., Helene,C. and Lavery,R. (1992) A computational and experimental study of the bending induced at a double-triple helix junction. *Biophys. Chem.*, **45**, 143–152.
17. Carbone,G.M., McGuffie,E., Napoli,S., Flanagan,C.E., Dembech,C., Negri,U., Arcamone,F., Capobianco,M.L. and Catapano,C.V. (2004) DNA binding and antigene activity of a daunomycin-conjugated triplex-forming oligonucleotide targeting the P2 promoter of the human c-myc gene. *Nucleic Acids Res.*, **32**, 2396–2410.
18. Vasquez,K.M., Dagle,J.M., Weeks,D.L. and Glazer,P.M. (2001) Chromosome targeting at short polypurine sites by cationic triplex-forming oligonucleotides. *J. Biol. Chem.*, **276**, 38536–38541.
19. Majumdar,A., Khorlin,A., Dyatkina,N., Lin,F.L., Powell,J., Liu,J., Fei,Z., Khripine,Y., Watanabe,K.A., George,J. *et al.* (1998) Targeted gene knockout mediated by triple helix forming oligonucleotides. *Nat. Genet.*, **20**, 212–214.
20. Asseline,U. and Thuong,N.T. (2001) Incorporation of halogenoalkyl, 2-pyridyldithioalkyl, or isothiocyanate linkers into ligands. In Beaucage,S.L., Bergstrom,D.E., Glick,G.D. and Jones,R.A. (eds), *Current Protocols in Nucleic Acid Chemistry*. John Wiley and Sons, Vol. 1, Chap. 4.8, pp. 1–13.
21. Asseline,U., Hau,J.F., Czernecki,S., Le Diguarher,T., Perlat,M.C., Valery,J.M. and Thuong,N.T. (1991) Synthesis and physicochemical properties of oligonucleotides built with either alpha-L or beta-L nucleotides units and covalently linked to an acridine derivative. *Nucleic Acids Res.*, **19**, 4067–4074.
22. Giovannangeli,C., Perrouault,L., Escude,C., Nguyen,T. and Helene,C. (1996) Specific inhibition of *in vitro* transcription elongation by triplex-forming oligonucleotide-intercalator conjugates targeted to HIV proviral DNA. *Biochemistry*, **35**, 10539–10548.
23. Faria,M., Wood,C.D., White,M.R., Helene,C. and Giovannangeli,C. (2001) Transcription inhibition induced by modified triple helix-forming oligonucleotides: a quantitative assay for evaluation in cells. *J. Mol. Biol.*, **306**, 15–24.
24. Alberti,P., Arimondo,P.B., Mergny,J.L., Garestier,T., Helene,C. and Sun,J.S. (2002) A directional nucleation-zipping mechanism for triple helix formation. *Nucleic Acids Res.*, **30**, 5407–5415.

25. Brunet,E., Alberti,P., Perrouault,L., Babu,R., Wengel,J. and Giovannangeli,C. (2005) Exploring cellular activity of Locked Nucleic Acid-modified triplex-forming oligonucleotides and defining its molecular basis. *J. Biol. Chem.*, **80**, 20076–20085.
26. Charneau,P., Mirambeau,G., Roux,P., Paulous,S., Buc,H. and Clavel,F. (1994) HIV-1 reverse transcription. A termination step at the center of the genome. *J. Mol. Biol.*, **241**, 651–662.
27. Diviacco,S., Norio,P., Zentilin,L., Menzo,S., Clementi,M., Biamonti,G., Riva,S., Falaschi,A. and Giacca,M. (1992) A novel procedure for quantitative polymerase chain reaction by coamplification of competitive templates. *Gene*, **122**, 313–320.
28. Asensio,J.L., Lane,A.N., Dhesi,J., Bergqvist,S. and Brown,T. (1998) The contribution of cytosine protonation to the stability of parallel DNA triple helices. *J. Mol. Biol.*, **275**, 811–822.
29. Kurreck,J., Wyszko,E., Gillen,C. and Erdmann,V.A. (2002) Design of antisense oligonucleotides stabilized by locked nucleic acids. *Nucleic Acids Res.*, **30**, 1911–1918.
30. Giovannangeli,C., Rougee,M., Garestier,T., Thuong,N.T. and Helene,C. (1992) Triple-helix formation by oligonucleotides containing the three bases thymine, cytosine, and guanine. *Proc. Natl Acad. Sci. USA*, **89**, 8631–8635.
31. Shiraishi,T. and Nielsen,P.E. (2004) Down-regulation of MDM2 and activation of p53 in human cancer cells by antisense 9-aminoacridine-PNA (peptide nucleic acid) conjugates. *Nucleic Acids Res.*, **32**, 4893–4902.
32. Grigoriev,M., Praseuth,D., Robin,P., Hemar,A., Saison-Behmoaras,T., Dautry-Varsat,A., Thuong,N.T., Helene,C. and Harel-Bellan,A. (1992) A triple helix-forming oligonucleotide-intercalator conjugate acts as a transcriptional repressor via inhibition of NF kappa B binding to interleukin-2 receptor alpha-regulatory sequence. *J. Biol. Chem.*, **267**, 3389–3395.
33. Neidle,S. and Thurston,D.E. (2005) Chemical approaches to the discovery and development of cancer therapies. *Nat. Rev. Cancer*, **5**, 285–296.
34. François,J.-C., Faria,M., Perrin,D. and Giovannangeli,C. (2004) DNA and RNA cleavage mediated by phenanthroline-cuprous oligonucleotides: from properties to applications. In Zenkova,M. A. (ed.), *Nucleic Acids and Molecular Biology—Artificial Nucleases*. Springer-Verlag, Germany, Vol. 13, pp. 223–242.
35. Arimondo,P.B., Boutorine,A., Baldeyrou,B., Bailly,C., Kuwahara,M., Hecht,S.M., Sun,J.S., Garestier,T. and Helene,C. (2002) Design and optimization of camptothecin conjugates of triple helix-forming oligonucleotides for sequence-specific DNA cleavage by topoisomerase I. *J. Biol. Chem.*, **277**, 3132–3140.
36. Brown,P.M., Madden,C.A. and Fox,K.R. (1998) Triple-helix formation at different positions on nucleosomal DNA. *Biochemistry*, **37**, 16139–16151.
37. Whitehouse,I., Stockdale,C., Flaus,A., Szczelkun,M.D. and Owen-Hughes,T. (2003) Evidence for DNA translocation by the ISWI chromatin-remodeling enzyme. *Mol. Cell Biol.*, **23**, 1935–1945.